Journal of
Mechanical
Science and
Technology

Journal of Mechanical Science and Technology 21 (2007) 559~567

A Quality Control Method by Ultrasonic Vibration Energy and Diagnosis System at Trimming Process

Shin-Jeong Kang[a,*], Mamoru Tanahashi[b], Toshio Miyauchi[b]

[a]*Seocho Technology Appraisal Center, Kibo Technology Fund*
[b]*Department of Mechanical and Aerospace Engineering, Tokyo Institute of Technology, Tokyo, Japan*

(Manuscript Received May 17, 2006; Revised December 5, 2006; Accepted January 15, 2007)

Abstract

To investigate a relation between vortex clusters and large-scale structures in the outer layer of wall turbulence, direct numerical simulations of turbulent channel flows have been conducted up to Re = 1270. The vortex clusters in the outer layer consist coherent fine scale eddies (CFSEs) of which diameter and maximum azimuthal velocity are scaled by the Kolmogorov length and the Kolmogorov velocity. The CFSE clusters are inside the large-scale structure, which contributes to the streamwise velocity deficit. The scale of those clusters tends to be enlarged with the increase of a distance from the wall. The CFSE clusters are composed of the relatively strong CFSEs, which play an important role in the production of the Reynolds shear stress and the dissipation rate of the turbulent kinetic energy. The most expected maximum azimuthal velocity of the CFSEs in these low-momentum regions of the outer layer is 30 ~ 70% faster compared with those of the CFSEs in unconditioned regions (*i.e.* all regions of the outer layer), while the most expected diameter of the CFSEs is not changed greatly.

Keywords: Turbulent channel flow; Direct numerical simulation; Large-scale structure; Coherent fine scale eddy

1. Introduction

Structure of wall turbulence has been one of the most important subjects in turbulence research because it is directly related to a lot of practical applications (e.g. drag reduction, heat transfer). In order to understand the dominant structure including streamwise vortices near the wall, many studies have been conducted for near-wall turbulence (Robinson 1991; Heist et al., 2000; Soldati 2000; Brooke et al., 1993; Jeong et al., 1997; Lyons et al., 1989). The streamwise vortices are elongated in the edge of the low-speed streak and kinked above it in the near-wall region. These streamwise vortices create a shear layer by pumping low-momentum fluid from the wall (Heist et al., 2000), and the generation of those is associated with changes in the shape of the low-speed streak surface (Soldati, 2000). Brooke et al. (1993) have argued that the new streamwise vortex is created at the wall in the downwash of a large stress-producing eddy by using velocity vector map on a x-z plane (in the present study, x, y and z axes represent streamwise, wall-normal and spanwise directions, respectively) and there is no strong interaction between the wall flow and the outer flow because the stress-producing eddies regenerate themselves. However, the streamwise vortices near the wall are stretched into the outer layer and a lot of hairpin-type vortices in the logarithmic region are connected to the streamwise vortices in the near-wall region (Tanahashi et al., 2004; Adrian et al., 2000).

*Corresponding author. Tel.: +82 2 2676 0941
E-mail address: kang73kang@yahoo.co.kr

The streaky structures are observed not only in the near-wall region but also in the outer layer, and the lateral spacing between low-momentum regions depends on the distance from the wall and varies with Reynolds number (Tanahashi et al., 2004). The spanwise wavelengths of the maxima in pre-multiplied energy spectrum of streamwise fluctuating velocity (u') are linearly increased in the logarithmic region of turbulent boundary layer (Christensen et al., 2001; Tomkins et al., 2003) and turbulent channel flows (Jimenez, 1998; Alamo et al., 2003). The increase of these spanwise wavelengths is caused by the low-speed streak existing in the logarithmic region, and results in the large-scale motion in wall turbulence. From particle image velocimetry (PIV) measurements on x-y planes in turbulent boundary layers, Meinhart & Adrian (1995) have observed growing zones of uniform low-momentum regions in the logarithmic region. These large-scale structures are physically important because they have long lifetime and occupy large volumes in the outer layer. Adrian et al. (2000) have proposed a model based on packets of hairpin vortices from PIV measurements on x-y planes in zero-pressure gradient boundary layers. They have also shown that the packets of hairpin vortices frequently occur, and coherent packets of the hairpin vortex heads appear throughout the logarithmic region. More recently, Tomkins & Adrian (2003) have suggested that the dominant large-scale motions are low u-momentum regions elongated in the streamwise direction, and the low-momentum regions are consistently associated with vortical motions at each height of y^+. However, the features of vortical motions and vortex clusters embedded in the low-momentum regions have not been investigated clearly.

From direct numerical simulation (DNS) results of turbulent flows, it has been shown that turbulence is composed of universal fine scale eddies (i.e. coherent fine scale eddies, hereafter CFSEs) which are verified in homogeneous isotropic turbulence, turbulent mixing layer and turbulent channel flows (Tanahashi et al., 2004; Jimenez et al., 1998; Tanahashi et al., 1999a; Tanahashi et al., 2001). The characteristics of the CFSEs at low- and high-Reynolds number cases can be scaled by the Kolmogorov length ( ) and Kolmogorov velocity (u_k) in homogeneous isotropic turbulence [up to Re 220 (Miyauchi et al., 2002)], turbulent mixing layer [up to Re =1300 (Tanahashi et al., 2001)] and turbulent channel flows [up to Re =800 (Tanahashi et al., 2004)]. However, the large scale range of the CFSEs increases with Reynolds number increase (Miyauchi et al., 2002). In turbulent channel flows, well-known streamwise vortices possess the same feature as the CFSEs (Tanahashi et al., 2004), which tend to be located between the low- and high-speed streaks in the near-wall region. From the analysis of DNS data of turbulent channel flows, our previous studies (Tanahashi et al., 2004; Kang et al., 2004) have shown that the large-scale low-momentum regions are deeply related with clusters of the CFSEs (hereafter CFSE clusters). It has been inferred that these clusters also include the structure similar to the packets of hairpin vortices proposed by Adrian et al.(Adrian et al., 2000). From PIV measurements on $x-y$ planes of turbulent boundary layer, Christensen & Adrian (2001) have statistically verified that the hairpin vortex packets exist in wall turbulence. Ganapathisubramani et al. (2003; 2005), who have performed stereoscopic and dual-plane PIV measurements on x-z planes of turbulent boundary layers, have developed a feature identification algorithm to search for both individual hairpin vortices and packets of hairpins. From the results based on this algorithm, they have reported that hairpin packets contribute more than 25% of total Reynolds shear stress even though they occupy less than 4% of the total area.

In the present study, DNSs of turbulent channel flows up to Re =1270 have been performed. From these DNS data, the CFSEs are educed to investigate a relation between the CFSE clusters and the low-momentum regions in the outer layer. The characteristics of CFSEs and turbulent statistics in the low- and high-momentum regions are also investigated with conditional probability density function.

2. DNS database

DNSs of turbulent channel flows have been performed by solving incompressible Navier-Stokes equations and continuity equation. Spectral methods are used in the streamwise and spanwise directions, and the central finite difference method with fourth-order accuracy is used in the wall-normal direction. The aliasing errors in the streamwise and spanwise directions are completely removed by using the 3/2 rule proposed by Orszag (1971). Periodic boundary conditions are used in the streamwise (x) and spanwise (z) directions for velocity and pressure fields, and the no-slip condition is applied in the wall-normal direction (y). DNS database and the other

computational information refer to Kang et al. (2006).

Figure 1 shows profiles of the mean streamwise velocity ($\overline{u}$) for all Reynolds number cases, which has already been printed in Kang et al. (2006). The solid and dashed lines in Fig. 1 represent the log and linear law, respectively. There are roughly two regions, i.e. near-wall region (I) and outer layer (II). Curves in y^+>40 for Re =400, 800 and 1270 correspond with the solid line (log-law curve), and wake regions are clearly observed in approximately y^+>200 (Re =400) ~ 450 (Re =1270). Namely, the outer layer can be classified as the logarithmic and wake regions.

3. Identification of coherent fine scale eddies

To investigate scaling law of the CFSEs up to Re =1270 and a relation between the CFSE clusters and the low-momentum regions in the outer layer, it is necessary to identify a method for extracting vortices from instantaneous turbulent flow field. The high vorticity or enstrophy regions have been widely used to identify coherent structures and vortical structures (Jimenez et al., 1998; Hussain et al., 1987; She et al., 1990). However, vorticity magnitude is not always appropriate for identification of vortical structures in turbulent channel flows, since high vorticity regions represent tube-like and sheet-like structures and they exist everywhere near the wall simultaneously (*i.e.* for the case with a strong background shear). Figure 2 shows the iso-surfaces of the second invariant (Q) of the velocity gradient tensor for Re =1270. The second invariant of the velocity gradient tensor is given by Q (=($_{ij}$ $_{ij}$ - $S_{ij}S_{ij}$)/2), where S_{ij} (=(u_i/x_j + u_j/x_i)/2) and $_{ij}$ =(u_i/x_j - u_j/x_i)/2) are the symmetric and antisymmetric parts of the velocity gradient tensor A_{ij} (= u_i/x_j = $_{ij}$ + S_{ij}). Figure 2 indicates that turbulent channel flow consists of a lot of tube-like structures similar to homogeneous isotropic turbulence (Tanahashi et al., 1999a), turbulent mixing layer (Tanahashi et al., 2001) and turbulent channel flows with low Reynolds number (Tanahashi et al., 2004; Kang et al., 2004). The density of the tube-like structures for high Reynolds number case is higher than that of lower Reynolds number cases in the unit cube of ^{3}. Streamwise vortices in the near-wall region and hairpin-type vortices can be visualized with the positive Q region. However, this visualization method depends on the threshold value of the variables. Therefore, Tanahashi et al. (2004; 1999a; 2001) have developed a new identification method which can educe fine scale eddies in turbulent flows without any threshold. This identification method is based on a local flow pattern, and the educed section includes a local maximum of Q. Furthermore, three-dimensional structure of the CFSE (or axis of the CFSE) is also identified by using an axis tracing method (Tanahashi et al., 2004) based on distributions of the positive Q region and the local flow pattern. More details about the identification method and the axis tracing method can be obtained in Tanahashi et al. (2004).

Figure 3 shows probability density functions (pdfs) of the diameter (D) and maximum azimuthal velocity ($V_{,max}$) of the CFSEs for Re =1270. These pdfs are calculated in several regions at different y^+. The diameter of the CFSE is defined as the distance between the locations where the mean azimuthal

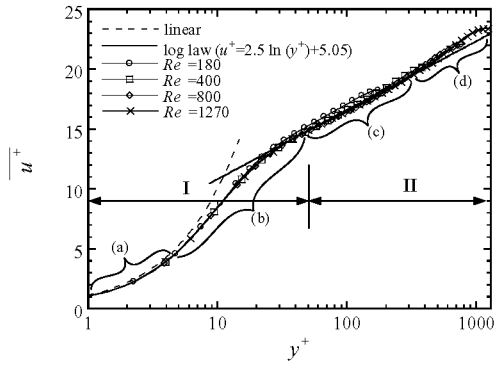

Fig. 1. The distributions of the mean streamwise velocity for all Reynolds number cases. I: near-wall region, II: outer layer (logarithmic (a) and wake (b) regions).

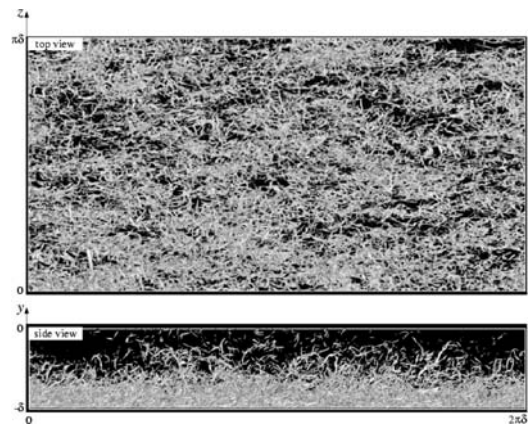

Fig. 2. Contour surfaces of the positive second invariant (Q) of the velocity gradient tensor for Re =1270 (Q=25, domain size: l_x l_y l_z = 2).

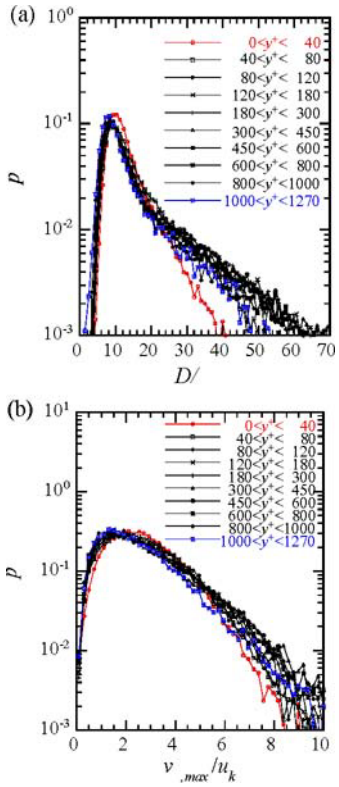

Fig. 3. Probability density functions of diameter (a) and maximum azimuthal velocity (b) of the CFSEs for Re = 1270.

velocity shows the maximum or minimum value. The diameter and maximum azimuthal velocity are normalized by and u_k, where and u_k are calculated from the mean dissipation rate ($\bar{}(y$)) of the turbulent kinetic energy at y^+. Tanahashi et al.(2004) have verified that the CFSEs can be scaled by and u_k in turbulent channel flows up to Re =800. In the near-wall region (y^+ <40), the most expected D and $V_{,max}$ are about 10 and 2.0 u_k, whereas they become about 8~9 and 1.2~1.8 u_k away from the wall. In the wake region near the center of the channel, the most expected D and $V_{,max}$ are about 8 and 1.2u_k, which are very close to the values in other turbulent flows (Tanahashi et al., 1999a; 2001). These results indicate that the CFSEs in turbulent channel flows can be scaled by and u_k up to Re =1270.

4. CFSE clusters and low-momentum regions

Figure 4 (a)~(d) show spatial distributions of the axes of the CFSEs for all Reynolds numbers. Figure 4 (b) and (c) represent two different regions with different

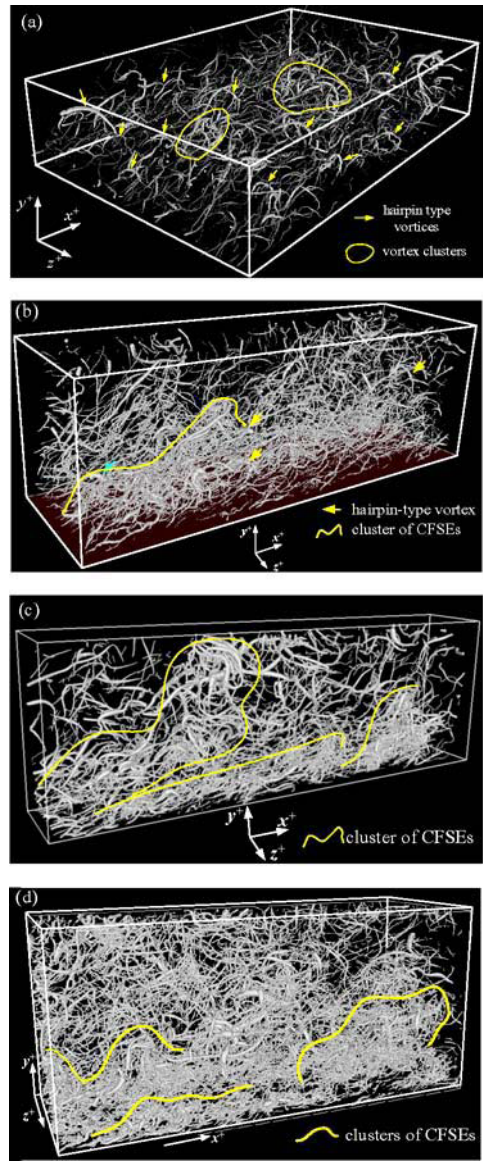

Fig. 4: Spatial distributions of the axes of the CFSEs for Re =400, 800 and 1270. Diameters of the axes are drawn to be proportional to the square root of Q^*. (a): Re =400, domain size: l_x l_y l_z 1884 400 1256 , (b) and (c): Re =800, domain size: l_x l_y l_z 2513 800 780 (b) and l_x l_y l_z 2513 800 400 (c), (d): Re =1270, domain size: l_x l_y l_z 2800 1270 1000.

spanwise width for Re =800. Their diameters are drawn to be proportional to the square root of Q^* on the axes, where Q^* is normalized by and u_k at y^+ (i.e. Q^* = Q /(u_k/)^2). Since the CFSEs in turbulent channel flows are scaled by and u_k, the vortical

structures can be visualized very well even in the regions far from the wall. These spatial distributions provide an evidence of the existence of hairpin-type vortices and groups of the CFSEs in the outer layer. In the cases of Re_τ=800 and 1270, the CFSE clusters are clearly observed because the logarithmic region is wider than that of Re_τ=400. In this study, the CFSE clusters are just defined as aggregate of the CFSEs which are educed by the axis tracing method. The number density of the CFSE clusters between the near-wall region and y/δ=0.5 is higher than that of the CFSE cluster in y/δ>0.5, and the CFSE cluster in the bottom of the logarithmic region is elongated in the downstream direction.

From the PIV measurements on x-z planes in turbulent boundary layer, Tomkins et al. (2003) and Ganapathisubramani et al. (2003) have shown that the low u-momentum regions, which are enveloped by positive and negative vortex cores and involve the packets of the hairpin vortex, are the dominant large-scale motions in the logarithmic region. Figure 5 shows spatial distributions of the axes of the CFSEs with iso-surfaces of u'^+ for Re_τ =400 and 800. The threshold values of the iso-surfaces in Fig. 5 (a) and (c) are selected to be equal to u'^+_{rms} at y 0.5δ. The low-momentum regions in the outer layer are composed of the CFSE clusters, which is independent of Re_τ considered in this study. The regions marked by circles in Fig. 5 (a) and (c) are enlarged in Fig. 5 (b) and (d) in order to show a relation between the high-/low-momentum regions and the CFSE clusters in the outer layer in detail. From these visualizations, one can clearly observe that the CFSE clusters are embedded in the low-momentum regions which are surrounded by the high-momentum regions. In wall turbulence, a lot of previous studies have reported that the typical lengthscales of these low-momentum regions in the logarithmic region vary from about δ to 3δ in the streamwise direction (Tomkins et al., 2003; Jimenez, 1998; Alamo et al., 2003; Townsend, 1976; Falco, 1977). These lengthscales are similar to those of the cluster structures observed in the present study.

To investigate a relation between the streaky structures and the CFSEs in the outer layer quantitatively, conditional probability density functions of u_c^* (=$u_c'^+$ (x^+, y^+, z^+)/ u'^+_{rms} (y^+)) are plotted for Re_τ =800 and 1270 in Fig. 6. Here, $u_c'^+$ (x^+, y^+, z^+) is the streamwise fluctuating velocity at the centers of the CFSEs. The pdfs are conditioned by the values of Q_c^* which is less than or greater than $Q_c^*(y^+)$. Here an

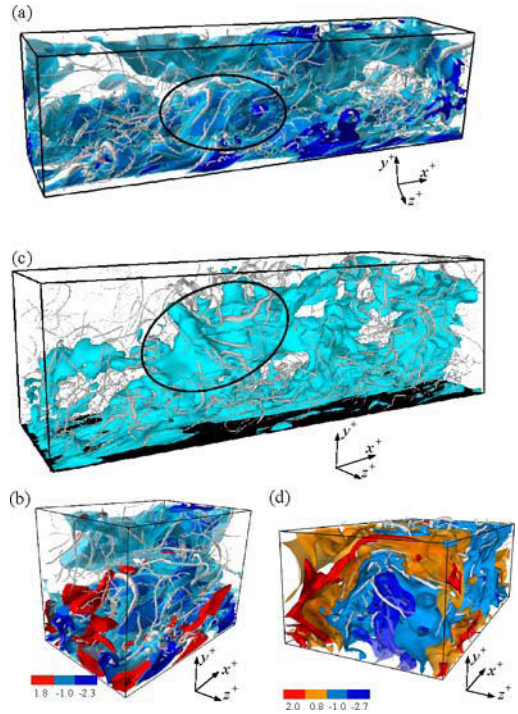

Fig. 5: Spatial distributions of the axes of the CFSEs with iso-surfaces of u'^+ for Re_τ =400 (a, b), 800 (c, d). The diameters of the axes are drawn by the same method as in Fig. 4. Visualized domain sizes: $l_x^+ \times l_y^+ \times l_z^+$ =1500×400×350 (a), x^+=400~900, y^+=0~400 and z^+=0~350 (b), $l_x^+ \times l_y^+ \times l_z^+$ = 2513×800×713 (c), x^+=628~2513, y^+=295~800, z^+=0~713 (d).

over-bar denotes mean value in x-z plane with y^+. Pdfs for $Q_c^* < \bar{Q}_c^*(y^+)$ show peaks around zero, whereas the peaks of pdfs for $Q_c^* \geq \bar{Q}_c^*(y^+)$ shift to the low-speed region (about u_c^* -0.5). Large portion of the CFSEs exists in the low-momentum regions ($u^* \leq$ -1.0) in the outer layer. This tendency is clearly observed for $Q_c^* \geq Q_c^*(y^+)$, which is also independent of the Reynolds number considered in this study. These results suggest that the low-momentum regions of $u' \leq -u'_{rms}$ in the outer layer consist of many CFSEs or CFSE clusters with relatively strong swirling motions. Since the CFSEs near the wall have the same features as the streamwise vortices and are generally located in the edge of the low- and high-momentum regions, the above result can not be extended to the near-wall region.

To visualize the relationship between the CFSEs and the low-momentum region at each height, iso-surfaces of streamwise fluctuating velocity normalized by the *rms* value at each height ($u^* = u'^+$

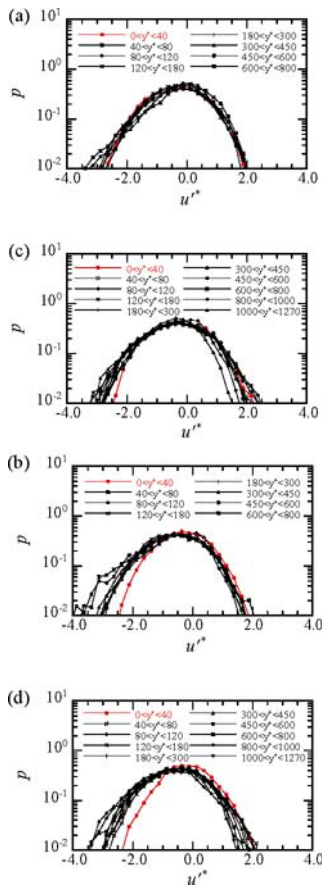

Fig. 6. Conditional probability density functions of u_c^* on the axes of the CFSEs. (a) and (b): Re_τ=800, (c) and (d): Re_τ=1270. (a) and (c): $Q_c^* < \overline{Q}_c^*(y^+)$, (b), (d): $Q_c^* \geq \overline{Q}_c^*(y^+)$. Q_c^* is normalized by η and u_k at y_c^+, and u_c^* is normalized by u_{rms} at y_c^+.

$(x^+, y^+, z^+) / u'^+_{rms}(y^+)$) are shown in Fig. 7 with axis distributions of the CFSEs for Re_τ =800. Here the thresholds of u^* are selected to 1.0 and -1.0, respectively. Three interesting regions including the CFSE cluster in Fig. 3 (b) are vi-sualized in Fig. 7. The low-momentum regions below about $-u_{rms}$ exist throughout the outer layer, and the inside of these low-momentum regions is composed of the CFSE cluster [see the I region in Fig. 7 (a)]. A large-scale low-momentum region in the wake region (y^+>300 for Re_τ=800) consists of a group of the CFSEs which are elevated from the logarithmic region. However, the number density of the CFSEs composing the clusters in the wake region is much lower than that in the logarithmic region. This will be discussed in the next section in more detail. On the other hand, there is

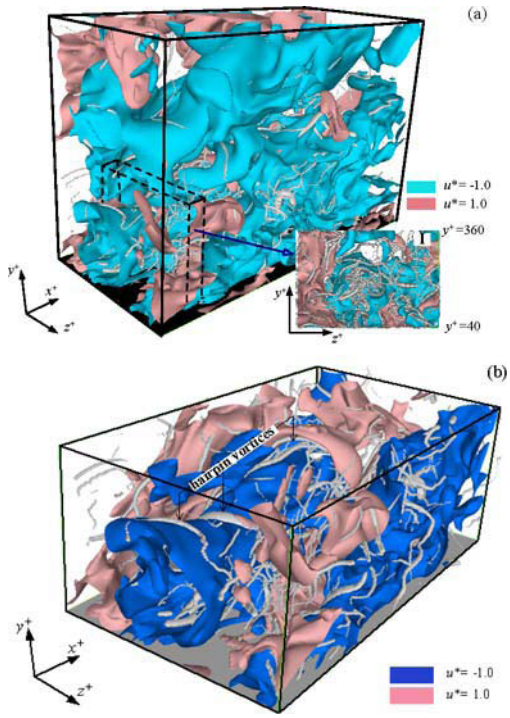

Fig. 7. Low- and high-momentum regions with the CFSE axes for Re_τ=800. Visualized domains are (a): x^+ = 0 ~ 1200, y^+ = 40 ~ 860 and z^+ = 200 ~ 780, (b): x^+ = 0 ~ 940, y^+ = 40 ~ 400 and z^+ = 200 ~ 780, respectively.

no CFSE cluster in the high-momentum region ($u^* \geq$ 1.0) in the outer layer. The cluster structures shown in Fig. 7(b) and Fig. 5(b) are very similar to the conceptual scenario (packets of hairpin vortices) proposed by Adrian et al. (2000). It should be noted that the cluster of the CFSEs dose not always possess hairpin packets type structure. Another possible structure in the logarithmic region is a bundle of the streamwise CFSEs.

Figure 8 shows the mean Reynolds shear stress ($-u'^+ v'^+$) and the dissipation rate of the turbulent kinetic energy ($\varepsilon^+ = 2\nu \overline{S'_{ij} S'_{i,j}}$) conditioned by u^*. The mean values without the condition are also plotted for comparison. In the outer layer, the mean Reynolds shear stress in low-momentum regions ($u^* \leq$ -1.0), which corresponds to ejection events (u'^+<0.0 and u'^+>0), shows very large values and the turbulent kinetic energy is dissipated extensively. The high-momentum regions of u^*>1.0, which corresponds to sweep events (u'^+>0.0 and u'^+<0), also produce a significant amount of the Reynolds shear stress, whereas the energy dissipation rate in those regions shows the small value.

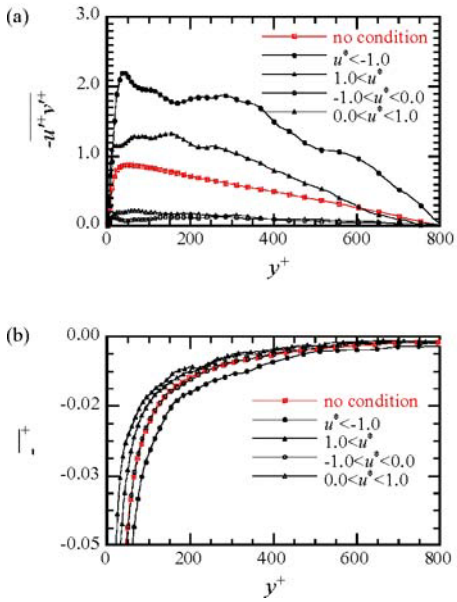

Fig. 8: Mean Reynolds shear stress (a) and mean dissipation rate of the turbulent kinetic energy (b) conditioned by u^* for Re =800.

5. Characteristics of coherent fine scale eddies in the low-momentum regions

From the axis distributions of the CFSEs with iso-surfaces of u^*, it has been observed that the CFSEs are scarcely clustered in the high-momentum regions (u^*>1.0) and there are a few CFSEs. On the other hand, the CFSEs in the low-momentum regions (u^*<-1.0) tend to possess relatively strong rotation rate and form clusters in the outer layer. In this section, characteristics of the CFSEs in the low-momentum regions are investigated for all Reynolds number cases by using pdfs of the diameter and maximum azimuthal velocity of the CFSEs conditioned by u^*. Figs. 9 and 10 show pdfs of the diameter and maximum azimuthal velocity of the CFSEs in the high- and low-momentum regions, respectively. The most expected diameter and maximum azimuthal velocity are about 10 and 1.0 ~ 1.5 u_k in the high-momentum regions, respectively. In the high-momentum regions far from the wall, the diameter and maximum azimuthal velocity of the CFSEs tend to become wider and weaker compared with those of the CFSEs without conditioning by u_c^* (the expected values in the whole flow field). However, the probabilities of the diameter and maximum azimuthal velocity in the low-momentum regions show peaks at

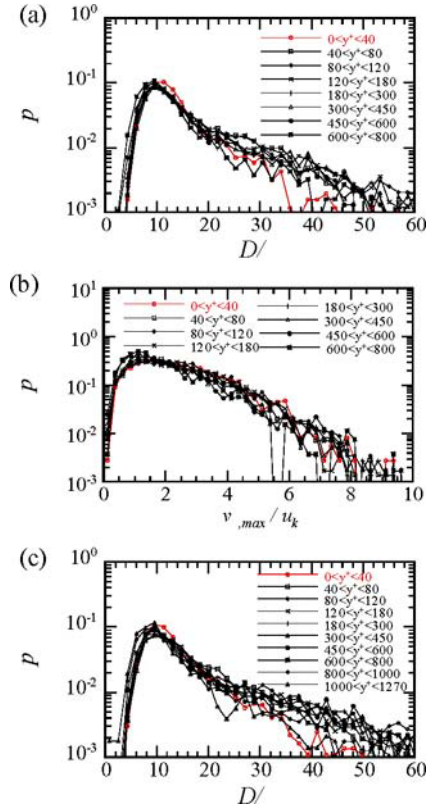

Fig. 9. Conditional probability density functions of diameter (a, c) and maximum azimuthal velocity (b, d) of the CFSEs in the high-momentum regions (u^* 1.0). (a) and (b): Re =800, (c) and (d): Re =1270.

about 8 and 1.5~2.5 u_k, respectively. In the low-momentum regions of the outer layer, the most expected diameter and maximum azimuthal velocity of the CFSEs are slightly narrower and 30~70 % faster than those of the CFSEs in the whole flow field. In particular, the most expected maximum azimuthal velocity of the CFSEs in the low-momentum regions is about 1.5~2.0 times of that in the high-momentum regions. These results are independent of the Reynolds number.

In the near-wall region, the probability of the diameter in both regions (i.e. high- and low-momentum regions) shows a peak at about 10 , whereas the maximum azimuthal velocity in the low-momentum regions is larger than that in the high-momentum regions for all Reynolds number cases. This result suggests that a lot of streamwise CFSEs are elongated at the edge of high- and low-speed streaks, but necks of the streamwise CFSEs (i.e. upper parts of streamwise vortices kinked spanwise direction) tend to be

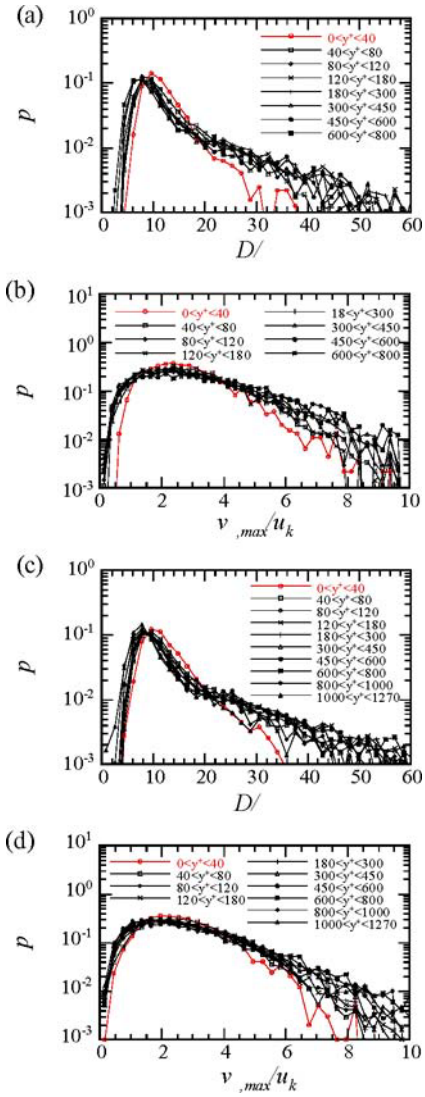

Fig. 10. Conditional probability density functions of diameter (a, c) and maximum azimuthal velocity (b, d) of the CFSEs in the low-momentum regions (u^* —1.0). (a) and (b): Re =800, (c) and (d): Re =1270.

located in the low-momentum regions of u^*<-1.0.

6. Conclusions

In the present study, direct numerical simulations of turbulent channel flows have been performed to investigate the clusters of vortices and their dynamics in the outer layer. The diameter and maximum azimuthal velocity of the CFSEs can be scaled by and u_k up to Re =1270. In the near-wall region (y^+<40), the most expected diameter and maximum azimuthal velocity are about 10 and 2.0u_k, whereas they become about 8 and 1.2u_k in the wake region near the channel center. The most expected values of those show weak y^+-dependence and have a tendency to decrease monotonically with the increase of a distance from the wall in the logarithmic region. There are many clusters of the CFSEs in the outer layer of turbulent channel flows. The low-momentum regions contain the CFSE clusters in the outer layer, and these cluster structures stand up with an angle in vertical plane. In the outer layer, the probability of the CFSEs existing in the low-momentum regions ($u^* \leq$ -1.0) is higher than that of the CFSEs existing in the high-momentum regions (u^*>1.0), which is emphasized for the relatively strong CFSEs.

The mean Reynolds shear stress in the low-momentum regions of the outer layer shows very large values and the turbulent kinetic energy is dissipated extensively. The high-momentum regions in the outer layer also produce a large percentage of the Reynolds shear stress, whereas the energy dissipation rate in those regions shows the small value. This result suggests that the low-momentum region with the CFSE cluster structures play a very important role in the production of the Reynolds shear stress and the dissipation mechanism of the turbulent kinetic energy in turbulent channel flows. The low-momentum regions in the outer layer are composed of the CFSEs which have a slightly narrower diameter and much stronger swirling motion compared with those in the high-momentum region.

References

Adrian, R. J., Meinhart, C. D., Tomkins, C. D., 2000, "Vortex Organization in the Outer Region of the Turbulent Boundary Layer," *Journal of Fluid Mechanics*, Vol. 422, pp. 1~54.

Alamo, J. C., Jimenez, J., 2003, "Spectra of Very Large Anisotropic Scales in Turbulent Channels," *Physics of Fluids*, Vol. 15, pp. L41~L44.

Brooke, J. W., Hanratty, T. J., 1993, "Origin of Turbulence-Producing Eddies in a Channel Flow," *Physics of Fluids* A, Vol. 5, No. 4, pp. 1011~1022.

Christensen, K. T., Adrian, R. J., 2001, "Statistical Evidence of Hairpin Vortex Packets in Wall Turbulence," *Journal Fluid Mechanics*, Vol. 448, pp. 433~443.

Falco, R. E., 1977, "Coherent Motions in the Outer Region of Turbulent Boundary Layers," *Physics of Fluids*, Vol. 20, pp. S124~132.

Ganapathisubramani, B., Longmire, E. K., Marusic, I., 2003, "Characteristics of Vortex Packets in Turbulent Boundary Layers," *Journal of Fluid Mechanics*, Vol. 478, pp. 35~46.

Ganapathisubramani, B., Longmire, E. K., Marusic, I., Pothos, S., 2005, "Dual-Plane PIV Technique to Resolve Complete Velocity Gradient Tensor in a Turbulent Boundary Layer," *Experiments in Fluids*, Vol. 39, pp. 222~231.

Heist, D. K., Hanratty, T. J., Na, Y., 2000, "Observations of the Formation of Streamwise Vortices by Rotation of Arch Vortices," *Physics of Fluids*, Vol. 12, pp. 2965~ 2975.

Hussain, A. K. M. F., Hayakawa, M., 1987, "Eduction of Large-Scale Organized Structure in a Turbulent Plane Wake," *Journal of Fluid Mechanics*, Vol. 180, pp. 193~ 229.

Jeong, J., Hussain, F., Schoppa, W., Kim, J., 1997, "Coherent Structures Near the Wall in a Turbulent Channel Flow," *Journal of Fluid Mechanics*, Vol. 332, pp. 185~ 214.

Jimenez, J., 1998, "The Largest Scales of Turbulent Wall Flows," *Center for Turbulence Research Annual Research Briefs, Stanford University/NASA Ames Research*, pp. 137~154.

Jimenez, J., Wray, A. A., 1998, "On the Characteristics of Vortex Filaments in Isotropic Turbulence," *Journal of Fluid Mechanics*, Vol. 373, pp. 255~285.

Kang, S. -J., Tanahashi, M., Miyauchi, T., 2005, "Coherent Fine Scale Eddies and Large-Scale Structures in Wall Turbulence," *Advances in Turbulence X*, pp. 603~ 606.

Kang, S. -J., Tanahashi, M., Miyauchi, T., 2006, "Elliptic Features of Coherent Fine Scale Eddies in Turbulent Channel Flows," *Journal of Mechanical Science and Technology*, Vol. 20, No. 2.

Lyons, S. L., Hanratty, T. J., McLaughlin, J. B., 1989, "Turbulence-Producing Eddies in the Viscous Wall Region," *AIChE Journal*, Vol. 35, pp. 1962~1974.

Meinhart, C. D., Adrian, R. J., 1995, "On the Existence of Uniform Momentum Zones in a Turbulence Boun-dary Layer," *Physics of Fluids*, Vol. 7, pp. 694~ 696.

Miyauchi, T., Tanahashi, M., Iwase, S., 2002, "Coherent Fine Scale Eddies and Energy Dissipation Rate in Homogeneous Isotropic Turbulence up to $Re \approx 220$, Presented at IUTAM Symposium on Reynolds Number Scaling in Turbulent Flow."

Orszag, S. A., 1971, "Numerical Simulation of Incom-pressible Flows with Simple Boundaries," *Studies in Applied Mathematics*, Vol. 50, pp. 293~327.

Robinson, S. K., 1991, "Coherent Motions in the Turbulent Boundary Layer. Annual Review of Fluid Mechanics", Vol. 23, pp. 601~639.

She, Z. S., Jackson, E., Orszag, S. A., 1990, "Intermittent Vortex Structures in Homogeneous Isotropic Turbu-lence," *Nature*, Vol. 344, pp. 226~228.

Soldati, A., 2000, "Modulation of Turbulent Boundary Layer by EHD Flows," *ERCOFTAC Bulletin*, Vol. 44, pp. 50~56.

Tanahashi, M., Iwase, S., Miyauchi, T., 2001, "Appearance and Alignment with Strain Rate of Coherent Fine scale Eddies in Turbulent Mixing Layer," *Journal of Tur-bulence*, Vol. 2, No. 6.

Tanahashi, M., Kang, S.-J., Miyamoto, T., Shiokawa, S., Miyauchi, T., 2004, "Scaling Law of Fine Scale Eddies in Turbulent Channel Flows up to Re =800," *Interna-tional Journal of Heat and Fluid Flow*, Vol. 25, pp. 331~ 340.

Tanahashi, M., Miyauchi, T., Ikeda, J., 1999a, "Identification of Coherent Fine Scale Structure in Turbulence," *Simulation and Identification of Organized Structures in Flow*, pp. 131~140.

Tomkins, C. D., Adrian, R. J., 2003, "Spanwise Structure and Scale Growth in Turbulent Boundary Layers," *Journal Fluid Mechanics*, Vol. 490, pp. 37~74.

Townsend, A. A., 1976, "The Structure of Turbulent Shear Flow," *2nd ed. Cambridge University Press*.